

**Climatic signature of two mid–late Holocene fluvial incisions formed under sea-level highstand conditions (Pisa coastal plain, NW**

**Tuscany, Italy)**

G. Sarti a,\*, V. Rossi b, A. Amorosi b, M. Bini a, S. Giacomelli a, M. Pappalardo, C. Ribecai a, A. Ribolini a, I. Sammartinob

a Department of Earth Science, University of Pisa, Pisa, Italy

b Department of Biological, Geological and Environmental Sciences, University of Bologna, Italy

**Abstract**

A multi-proxy (stratigraphic, geomorphological, palynological, geophysical) study of mid–late Holocene deltaic–alluvial deposits beneath the Pisa Plain (Tuscany, Italy) reveals short-term enhances of fluvial activity under relative sea-level highstand (HST) conditions (last ~7000 cal yr BP). Early HST delta progradation led to the progressive infill of a broad lagoon area (~5000 cal yr BP), followed by the development of a stable alluvial depositional environment (~4000 cal yr BP). The intense phase of alluvial aggradation was punctuated by two events of enhanced fluvial incision that cut down to 10m the underlying lagoonal substrate. The two erosive events, which reflect centennial-scale changes in the aggradation/degradation ratio, are chronologically constrained to the Eneolithic–Bronze age transition (~3800 cal yr BP) and to the Bronze–Iron age transition (2900–2800 cal yr BP), respectively. A detailed pollen profile highlights the correlation between these erosive events and two phases of increased humidity (Abies peaks 1 and 2) recorded in several sites of Europe. This correlation suggests a key-role of climate fluctuations in triggering channel incision. The peculiar high compressibility of the lagoonal substrate can also have acted as a factor able to foster the deepening of the channels. In contrast, the role of relative sea-level changes and human impact on the activation of the two erosive processes appears negligible.

**1. Introduction**

Under long-term highstand sea-level conditions, the majority of depositional models agree with the development of aggradational to progradational deltaic–alluvial sequences, in which isolated, high sinuosity fluvial channels are cut through overbank fine-grained deposits (Posamentier et al., 1988; Catuneanu, 2006; Catuneanu et al., 2009). However, in Quaternary successions the complex interplay of regional (sea-level, climate), local (geological and tectonic setting, physiography) and human-induced forcing factors may strongly influence river activity on a sub-Milankovitch scale, inducing high frequency changes in sedimentation patterns (Starkel, 1983, 2000; Maddy et al., 2001; Benito et al., 2003; Lewin et al., 2005; Jones et al.,

2010; Macklin et al., 2012; Turner et al., 2013).

In this regard, the deltaic–alluvial successions formed during the mid–late Holocene period (ca. the last 8000–7000 cal yr BP) under decelerating sea-level rise (less than 1 mm yr<sup>-1</sup>; Stanley and Warne, 1994; Lambeck et al., 2004) and increasing sediment supply due to both anthropogenic and climatic factors represent valuable sedimentary archives for a detailed comprehension of fluvial system dynamics and a pertinent evaluation of the main driving factors (Posamentier et al., 1988; Somoza et al., 1998; Catuneanu, 2006). Although generally weaker in amplitude and magnitude than Lateglacial (Heinrich stadial 1, Bølling–Allerød interstadial and Younger Dryas) and last glacial (Dansgaard–Oeschger and Heinrich events) events (Alley et al., 2003; Hemming, 2004; Steffensen et al., 2008), the mid–late Holocene short-term climate oscillations (Mayewski et al., 2004; Wanner et al., 2008; Helama et al., 2010) are proven to leave identifiable traces in the fluvial record. Across western and central Europe, slack water flood deposits provide a centennial-scale record of flood frequency increase, potentially correlative to mid–late Holocene climatic changes (Macklin and Lewin, 2003; Lewin et al., 2005; Macklin et al., 2006; Starkel et al., 2006; Thorndyraft and Benito, 2006).

Valuable insights on high-frequency fluvial dynamics–climate–land use interactions can be inferred through a multiproxy, high-resolution examination of the mid–late Holocene stratigraphy recorded beneath the subsiding Mediterranean coastal plains. Here, the abundance of fine-grained deposits, where pollen and traces of human occupation are well preserved, and the good chronological control offered by radiocarbon dates coupled with widespread archeological remains potentially make these highstand sedimentary wedges (Highstand Systems Tract-HST) a truly effective and powerful natural laboratory on which to infer the potential response of the coastal plain to future climatic variations due to both anthropogenic and natural causes.

In the Pisa coastal plain (NW Tuscany, Italy; Fig. 1A), located within

the southern portion of the extensional Viareggio Basin (Malinverno and Ryan, 1986; Martini and Sagri, 1993; Patacca et al., 1993; Pascucci, 2005), the mid-late Holocene deltaic-alluvial succession is remarkably thick (10–15 m; Amorosi et al., 2013a) and rests on a laterally extensive stratigraphic marker, composed of homogeneous, soft lagoonal clays deposited during the late transgressive-early highstand phases (ca. 8000–5000 cal yr BP-Neolithic age in Table 1; Benvenuti et al., 2006; Rossi et al., 2011; Amorosi et al., 2013a). The prograding deltaic-alluvial wedge is made up of swamp soft clays, which in turn are overlain by poorly drained floodplain clays chronologically constrained to the proto-historic period (Table 1; Amorosi et al., 2013a). These finegrained deposits are locally juxtaposed to crevasse splay/levee silty-sandy complex and fluvial sand bodies, deeply truncating the underlying succession (Sarti et al., 2012; Amorosi et al., 2013a) (Fig. 1). The overall vertical stacking pattern of facies in the Pisa Plain documents a typically progradational evolutionary trend that led to the formation of the modern deltaic and alluvial plains (Somoza et al., 1998; Amorosi and Milli, 2001; Vella et al., 2005; Fanget et al., 2014). In the Pisa urban area the establishment of a genuine alluvial depositional system was the result of the activity of the Arno River and a former branch of the Serchio River, known as Auser, flowing from the Pisa Mountains to the city (Fig. 1A–B). Up to the Etruscan age (ca. 2500–2000 cal yr BP; Table 1) these rivers were subjected to recurring processes of migration and avulsion favored by the very low gradients and high sinuosity (Amorosi et al., 2013a). This natural tendency was greatly thwarted by Roman waterworks and systematic land reclamation (Roman Centuriatio, starting from ca. 2000 cal yr BP), which led to the development of an extensive well-drained floodplain in the Pisa urban and suburban areas. Only during the Middle Ages (XI century; Bruni and Cosci, 2003) human intervention definitively forced the Auser outside the city walls.

This paper aims to improve our understanding of fluvial systems

evolution in relation to natural and human-induced changes during the mid–late Holocene, a crucial period in the evolution of modern Mediterranean alluvial and coastal plains. Interpretation was strengthened by correlation of high-resolution stratigraphic, geomorphological and shallow geophysics data along with on-site pollen and archeological records.

Specifically, we focus on the role of two deep fluvial incisions occurred in the Pisa area under relative sea-level highstand conditions, during the Bronze–Iron ages (between ca. 4000 and 2500 cal yr BP; Table 1).

## 2. Materials and methods

### 2.1. Stratigraphic data and analysis

The stratigraphic architecture of the Pisa Plain prograding sedimentary wedge was investigated by means of a dense grid of cross-sections, following the paths of the highest quality core data stored into the georeferenced subsurface dataset (Amorosi et al., 2013b) with maximum spacing of ~500 m (Fig. 2). Detailed facies characterization of the mid–late Holocene succession was performed through integrated sedimentological, geochemical, micropaleontological and palynological analyses (Amorosi et al., 2013a) carried out on the reference cores (continuously cored boreholes and percussion drilling cores), recently drilled during the MAPPa Project coring campaign (<http://www.mappaproject.arch.unipi.it>) in the Pisa urban and suburban area (Fig. 2). This multidisciplinary approach allowed the identification of seven lithofacies associations, essential for high-resolution stratigraphic correlations and reconstruction of sedimentary evolution. The lithofacies, described in detail by Amorosi et al. (2013a), are here summarized in Table 2, along with the main diagnostic sedimentological and paleontological features.

### 2.2. Remote sensing analysis

In the study area the stratigraphic reconstruction was refined through identification of the past fluvial landforms by integrated

techniques of remote sensing analysis (Bisson and Bini, 2012). Specifically, the analysis of multitemporal aerial photographs, ranging in age from 1943 to 2010, and multispectral images with medium–high resolution acquired from SPOT, ALOS AVNIR-2 and TERRA ASTER satellites allowed the identification of a series of prominent, shallow paleotracés (paleochannels) buried beneath the Pisa Plain.

In a key-portion of the study area, where the paleoArno and Auser merge as mentioned by Strabo (Fig. 1B), in order to reinforce the cross-reference between stratigraphic and morphological data a paleotrace was further investigated by 2D Electrical Resistivity Tomography (ERT) (Fig. 2). The ERT profile explored the uppermost 30 m from the ground level, adopting the roll-along acquisition technique, with electrodes spacing of 2 m. A Schlumberger and Wenner configuration combined with dipole–dipole array was used. The 2D inversions of apparent resistivity were undertaken using the TomoLab software ([www.geostudiastier.com](http://www.geostudiastier.com)).

### 2.3. Palynological analysis

Fifteen samples from clay and silt deposits of core M5 (Fig. 2 for location) were collected for palynological analysis. The presence of a thick, continuous fine-grained succession of lagoon, swamp and poorly-drained floodplain deposits (see Section 1), where pollen grains are expected to be well preserved, made M5 the reference core for the reconstruction of the pollen sequence. Within the lower portion of the core, between 10.5 and 6 m core depth, samples were taken at 20–40 cm intervals. Only two samples were collected from the uppermost part of the core, where pollen and spores are rare and badly preserved within crevasse splay sands and stiff, well-drained floodplain clays. Standard palynological techniques (HCl, HF, chemical treatment) for mineral dissolution were applied on 10 g of each sample (Fægri and Iversen, 1989). In order to preserve all the organic components, neither oxidative nor alkali treatments were applied. The concentration of pollen, spores and other palynomorphs is estimated by adding a tablet

containing a known amount of *Lycopodium* spores. At least 200 wellpreserved pollen and non-pollen palynomorphs were counted per sample, and the relative abundance of each taxa was calculated. Pollen taxa were identified according to the literature (Reille, 1992, 1995, 1998 and online databases, <http://www.europeanpollendatabase.net>) and grouped on the basis of their ecological and climatic affinities, following the indications of previous works carried out in the Arno coastal plain (Aguzzi et al., 2007; Ricci Lucchi, 2008; Amorosi et al., 2009).

Among the non-pollen palynomorphs the marine-related elements, including dinocysts, foraminiferal linings and scolecodonts, and the pteridophyte spores were identified (Traverse, 1988) providing further paleoenvironmental information. In addition, reworked pre-Quaternary elements were counted to highlight phases of intense fluvial activity.

#### 2.4. Chronology

The chronological framework of the studied succession benefited from 14 radiocarbon dates (Table 3) and scattered ceramic remains from the uppermost stratigraphic interval. AMS <sup>14</sup>C analyses were performed on wood fragments, organic matter and mollusc shells at CIRCE Laboratory of Caserta (Naples University). Conventional ages were calibrated using the CALIB5 program and the INTCAL09 or MARINE09 calibration curves (Reimer et al., 2009) for terrestrial and marine materials, respectively. In order to compensate for the reservoir effect, mollusc samples were calibrated using an average value of  $\Delta R$  ( $35 \pm 42$ ), estimated for the northern Tyrrhenian Sea from online databases (<http://calib.qub.ac.uk/marine/>). In this study, the ages are reported as the highest probability range (cal yr BP) obtained using two standard deviations- $2\sigma$  (Table 3).

### 3. Mid-late Holocene deltaic-alluvial sedimentation and channel dynamics

#### 3.1. Subsurface stratigraphic architecture

The mid-late Holocene deltaic-alluvial succession of the Pisa Plain records the gradual filling of a wide lagoon basin and the establishment

around 5000 cal yr BP of a delta system that was replaced by an alluvial plain one thousand years later (Fig. 3A–D; Amorosi et al., 2013a). In terms of sequence stratigraphy, this prograding sedimentary wedge represents the HST of the late Quaternary depositional sequence and displays, as a whole, the distinctive sedimentary signature of a high accommodation depositional setting (Miall, 1996; Catuneanu, 2006).

Indeed, the occurrence of isolated to locally amalgamated channel deposits within a dominantly fine-grained succession (Fig. 3A–D) reflects the cumulative effect of highstand relative sea-level conditions and tectonic subsidence experienced by the study area during the Holocene (Lambeck et al., 2004; Pascucci, 2005).

According to previous work (Rossi et al., 2012; Amorosi et al., 2013a), the lower portion of the deltaic–alluvial succession is made up of swamp clays, 1 to 3 m-thick, dated around 5000–4000 cal yr BP

(Eneolithic age; Tables 1, 3). Up to 2 m-thick subdelta and distributary channel sand bodies, with top at ~6 mbsl, locally interrupt the lateral continuity of the swamp layers (cores S1\_T, S1\_6P and M19 in Fig. 3C–D). However, isolated to locally amalgamated channel bodies up to 5–4 m-thick and with top-of sand at ~5 mbsl locally truncate the underlying swamp and lagoon succession down to 10 mbsl (Fig. 3A–D). These channel sands grade upwards into poorly-drained floodplain clays or levee/crevasse sandy deposits (Fig. 3A–D). Facies architecture integrated with the available radiocarbon ages constrains the timing of fluvial incision to the Eneolithic–Bronze age transition (around 4000–3800 cal yr BP in Table 1). Upwards, poorly-drained floodplain clays, up to 4 m-thick, show vertical and lateral transition to crevasse splay/levee and fluvial channel sands, whose upper boundaries mainly cluster around 4 m and 1 mbsl (Fig. 3A–D). Channel deposits with top-of-sand at ~4 mbsl form remarkably thick (up to 5–6 m) sand bodies, which further erode the floodplain–swamp–lagoon succession down to 10 mbsl. Radiocarbon and archeological data constrain the activity of these channels to the Bronze–Iron transition (around 2900–

2800 cal yr BP in Table 1).

In contrast, the channel bodies clustering at shallower depths (top-of-sand ~1mbsl) are thinner (~2m) and show lens-shaped geometries (core S5\_SC in Fig. 3C). Upwards, around the present sea level, poorly drained floodplain clays are overlain by well-drained floodplain silty clays dating back to the early Roman period (Fig. 3A–D and Table 1).

Crevasse splay/levee deposits and isolated fluvial-channel bodies, with top-of sand around or above the present sea level, are mainly recorded beneath the modern Arno River course (Fig. 3A, C–D). A different stacking pattern of fine-grained lithofacies characterizes the historical

Pisa city center, north of the modern Arno River course, where laterally extensive clay deposits formed in ephemeral and shallow backswamps

occur around 2 mbsl (Fig. 3A–D). Radiocarbon ages and several ceramic materials constrain the development of these low-lying wetlands to the late Iron–early Etruscan age (ca. 2500 cal yr BP/ca. 7th–5th century BC; Amorosi et al., 2013a). Anthropogenic structures, dated from the Roman period onwards, cut the alluvial succession at various stratigraphic levels.

### 3.2. Fluvial paleodrainage network

More than 10 distinct fluvial paleotracess were identified by remote sensing in the Pisa urban and suburban area (Fig. 4A), documenting the significant contribution of the fluvial network to the geomorphological evolution of the plain (Amorosi et al., 2013a).

Specifically, an east–west oriented paleochannel chronologically constrained to the Eneolithic–Bronze age transition (top-of-sand ~5 mbsl; Section 3.1. and Fig. 3A–D) was identified north of the modern Arno River (paleoArno; Fig. 4A). Consistent with Strabo's chronicles, a semi-coeval north–south oriented paleochannel flowing close to the west medieval city wall is referred to the Auser branch (paleoSerchio), which merged into the paleoArno close to the Arsenali area (Figs. 1 and 4A; Amorosi et al., 2013a). A further paleochannel, active during the Eneolithic–Bronze age transition was identified in the eastern portion



of the Pisa Plain with east–west flowing direction. On the basis of its position and orientation (see Figs. 1 and 4A), this paleochannel is interpreted as the Auser branch that flowed from the Pisa Mountains to the city area, running along the north medieval city wall before splitting into two or more branches as mentioned by the Greek geographer Strabo (Chronicles, V, 2, 5, C 222). Neither stratigraphic nor morphological data allow to recognize the westward prolongation of this paleochannel, which was likely connected with the north–south Auser branch in the Arsenali area.

Concerning the drainage network active at the Bronze–Iron transition and related to the second phase of rapid channel incision and fill (top-of-sand ~4 mbsl; Fig. 3C–D), two paleotracess were identified immediately south of the modern Arno River (Fig. 4A). These traces document the abrupt southward shift of the paleoArno and two rapid phases of meander migration (Figs. 3C, D and 4A). In contrast, no paleotracess potentially pertaining to the Auser River course were identified (Fig. 4). The ERT profile carried out along the north–south oriented Auser River paleotrace (Figs. 2 and 4A, B) reinforces our paleogeomorphological interpretation and traces out the geometry of the paleochannels involved in the first phase of rapid channel incision and fill.

Three sub-elliptical areas with high resistivity (300–1000  $\Omega$  m) are the most striking feature observed at 7–8 m depth (4–5 m ca. bsl) across the whole ERT section (4–5 m ca. asl, Fig. 4B). These areas show sharp contacts with the overlying low-resistivity layer and a progressive decrease in resistivity down to the lower limit of investigation (c.a. 14–15 m depth). Core S1\_exM drilled nearby enabled lithofacies calibration of the electrical resistivity data (Fig. 4C). The rapid increase in resistivity at 7–8 m is coherent with the boundary between floodplain clays and the underlying thick succession of fluvial–channel sands. The contouring of these high-resistivity sands shows a sub-elliptical shape that can be related to a fluvial channel cross-section. Close to the lower limit of ERT resolution (c.a. 12 m depth), the decrease of

resistivity fits with the sharp transition to clayey lagoon sediments.

In this respect, electrical resistivity data support the hypothesis that fluvial channels were carved into more conductive, fine-grained sediments.

#### 4. Mid–late Holocene pollen record

Samples from core M5 contain a rich, autochthonous palynological association mainly composed of pollen grains and spores. Other palynomorphs (algae, dinoflagellates, scolecodonts and foraminiferal linings) are recorded within lagoonal sediments in the lowermost part of the core. The state of preservation is generally good, with 3% indeterminable or unknown grains, while pollen concentration strongly fluctuates throughout the cored succession. Pollen concentration from lagoon sediments and the lowermost swamp succession varies from 13,434 to 16,126 grains/g. Within the overlying swamp clays, between 8.76 m and 8.60 m core–depth, the concentration abruptly drops to 4475 grains/g, and then further gradually decreases upwards. In contrast, pre-Quaternary palynomorphs generally exhibit an upward increasing trend in relative percentages with respect to the total autochthonous plus allochthonous assemblage.

Despite the overall dominance of arboreal pollen (AP), which is distinctive feature of the Holocene successions across the Mediterranean area (Bellini et al., 2009; Di Rita and Magri, 2012), high-frequency abundance changes of specific pollen groups (see Section 2.3) allow the distinction of four main pollen zones (1–4), corresponding to distinct vegetation phases (Fig. 5). These zones are described and interpreted in terms of past climatic conditions and environmental features, as follows (Fig. 5).

##### 4.1. Zone 1: 10.50–9.60 m

###### 4.1.1. Description

This zone is characterized by an autochthonous pollen association mainly composed of riparians (17–32%), almost entirely represented by *Alnus*, and deciduous/evergreen trees, such as *Quercus* and *Corylus*

(~5–15% and 6–9.5%, respectively). Both groups show decreasing upward trends. Mountain and Mediterranean trees are also present with remarkable percentages (6–8% and 4–10.5%, respectively — Fig. 5). The herbaceous taxa (NAP) are mainly represented by ubiquitous (up to ~31% at the top of the zone) and aquatic (~2–6%) plants. Among non-pollen palynomorphs, pteridophyte spores are the most abundant (~10–12.5%), while marine-related elements (dinocysts, foraminiferal linings and scolecodonts) show low percentages. Reworked pre-Quaternary palynomorphs (pollen grains and dinocysts) are very scarce throughout this zone, peaking at ~4% close to its upper boundary (Fig. 5). The most common components of this group are species of *Corollina* genus, an extinct pollen taxon commonly found within lower Mesozoic sequences in both hemispheres (Traverse, 1988).

#### 4.1.2. Interpretation

The high pollen concentration values and the scarce occurrence of reworked pre-Quaternary palynomorphs fit well with the development, in the Pisa Plain, of a wide lagoonal basin during the Neolithic age (Figs. 3 and 4), as recently documented by Amorosi et al. (2013a). The high abundance of *Alnus* and pteridophytes as well as the occurrence of marine-related palynomorphs are also consistent with this paleoenvironmental interpretation. Moreover, the presence of reworked *Corollina* specimens suggests sediment supplied by nonmetamorphic Mesozoic sedimentary sequences cropping out north of Pisa.

The occurrence of mixed deciduous/evergreen oak forests, similar to those characterizing the west coasts of Italy between ca. 8000 and 5000 cal yr BP (Amorosi et al., 2009; Ribecai, 2011; Di Rita and Magri, 2012) indicates optimal warm and humid climate conditions.

#### 4.2. Zone 2: 9.60–8.10 m

##### 4.2.1. Description

This zone is characterized by a significant drop in pollen concentration (from 16,126 to 4475 grains/g), paralleled by the upward decrease

of the AP/NAP ratio (~1) close to the upper boundary. The main character of the pollen association is the strong increase of riparians, mainly represented by *Alnus*, which peaks (~50%) close to the lower boundary of the zone and progressively decreases upwards (Fig. 5). Deciduous woody taxa (dominant *Ulmus* and subordinate *Quercus* and *Corylus*) are still present with considerable percentages (8–17%; Fig. 5). Mountain and Mediterranean trees invariably exhibit values lower than 5%.

Among the herbs, Poaceae display the highest percentages of the whole core (up to 25%; Fig. 5). The aquatic plants are abundant across the entire zone, with a distinct peak (~30.5%) close to its upper boundary, where pteridophytes also show very high percentages (~20%; Fig. 5).

Reworked pre-Quaternary palynomorphs, mainly represented by *Corollina* spp., slightly increase in concentration relative to the underlying zone 1, with 10% relative abundance at the upper boundary (Fig. 5).

#### 4.2.2. Interpretation

The rapid expansion of *Alnus*, a hygrophilous tree taxa requiring moist soils habitat (Di Rita and Magri, 2012) is consistent with the replacement of the lagoon by a vast wetland area around the Pisa city center at the transition to the Eneolithic age (around 5000 cal yr BP; Figs. 4 and 5; Amorosi et al., 2013a). The high percentages of both aquatic plants and pteridophytes in the uppermost portion of the pollen zone also testify to the progressive filling of the lagoon and to the establishment of distinct paludal conditions. Similarly, an upward increasing trend is shown by the reworked pre-Quaternary palynomorphs, reflecting the progressive influence of the drainage network at the core site area.

As a whole, the pollen association indicates the development of a marshland at the beginning of the Eneolithic age, rapidly followed by mixed woodlands and *Alnus* carrs, in accordance with other pollen

records from the west coast of Italy (Di Rita and Magri, 2012). Interestingly, in the upper portion of the zone our data clearly indicate the partial replacement of deciduous-*Alnus* forests by grasslands, mainly composed of Poaceae, aquatics and ferns (pteridophytes), and a strong decrease of mountain trees (Fig. 5). These vegetation changes and the concomitant drop of both AP/NAP ratio and pollen concentration point to a phase of forest reduction around 4200–4000 cal yr BP (radiocarbon ages in Fig. 5), reasonably related to a short-term climatic perturbation towards drier conditions. A comparable and semi-coeval event of forest decline (ranging between 4500 and 3900 cal yr BP in Europe) has been recently reported from several coastal sites of central-southern Italy (Drescher-Schneider et al., 2007; Magri, 2007; Di Rita et al., 2010; Sadori et al., 2011; Di Rita and Magri, 2012) and related to the temporary latitudinal displacement of the inter-tropical convergence zone. This deterioration of climate conditions appears to be contemporary with a well-known, global climate event centered around 4200 cal yr BP, the so-called 4.2 ka event or event 3 of Bond et al. (1997, 2001), widely recorded by several proxies across the Mediterranean area (Magny et al., 2002, 2009; Mayewski et al., 2004; Piva et al., 2008; Bar-Matthews and Ayalon, 2011; Giraudi et al., 2011; Zanchetta et al., 2013).

These paleoclimatic records offer a complex picture of the 4.2 ka event with latitudinal and longitudinal contrasting humidity conditions (Magny et al., 2012a,b), probably due to the combined effect of cyclonic activity and seasonal, local patterns, and suggest for the central Mediterranean area a close succession of events (wet/dry/wet) between 4300 and 3800 cal yr BP (Magny et al., 2009; Zanchetta et al., 2013).

#### 4.3. Zone 3: 8.10–6.50 m

##### 4.3.1. Description

This zone is characterized by an abrupt decrease of the riparian trees (b10%) and aquatic plants. This trend is paralleled by a strong increase in *Pinus* (up to ~27.5%), which becomes the dominant arboreal taxon, and

herbs, mainly represented by ubiquitous and steppic taxa (Fig. 5). Mixed oak woods (*Quercus*, *Corylus*, *Ulmus* and *Tilia*) occur as secondary taxa with remarkable percentages (7–10%), while the Mediterranean and mountain trees are generally present at very low values (4%; Fig. 5). Two anomalous samples close to the zone boundaries (~8 m and ~6.50 m core depth) show an increase of mountain trees (up to 10%), almost exclusively represented by *Abies* grains (*Abies* peaks 1 and 2 in Fig. 5). Reworked palynomorphs, derived from pre-Quaternary outcropping formations (*Corollina* spp., *Rhétipollis germanicus* and various Jurassic–Cretaceous dinoflagellates and spores) also peak within the same stratigraphic intervals, reaching the highest percentages of the whole cored succession (Fig. 5). Consistently, peaks of reworked dinocysts, foraminiferal linings and scolecodonts derived from the underlying lagoonal deposits cap the zone (~5%; Fig. 5).

#### 4.3.2. Interpretation

The high amounts of *Pinus* grains, strongly resistant to mechanical stress, and the increasing abundance of the herbaceous taxa (Fig. 5) reflect the establishment of a genuine alluvial landscape (Amorosi et al., 2013a) with sparsely wooded grasslands during the Bronze–Iron ages (Figs. 3 and 5). On shorter timescales, two peaks of reworked palynomorphs (both pre-Quaternary and lagoon-derived) are recorded close to the lower and upper boundaries of this zone, recording rapid, high-energy flood events (Fig. 5). In the same stratigraphic intervals, two peaks of *Abies* (*Abies* peaks 1 and 2 in Fig. 5) reveal short-lived phases of increasing moistness. Indeed, *Abies* grows and spreads under high-humidity conditions only (Tinner and Lotter, 2006; Mariotti Lippi et al., 2007; Ricci Lucchi, 2008), and is currently found as scattered communities in the Tuscan Apennines at elevations higher than 1000 m.

To date, no comparable proto-historic events of *Abies* expansion have been recorded from other Italian coastal sites, possibly due to a combined effect of local climate and high human pressure (Tinner et al., 2013; Di Pasquale et al., 2014). Unique exception is the pollen

record recovered from the near archeological site of Pisa S. Rossore (Fig. 1B), where remarkable percentages of drought-sensitive mountain trees (*Fagus* and *Abies*) have been encountered within the pre-Roman unit that overlies the Neolithic lagoon clays (Mariotti Lippi et al., 2007). Unfortunately, the available radiocarbon ages do not furnish a more precise chronological framework for this unit.

Nevertheless, our observations are in general agreement with the multi-proxy evidence of millennial to centennial-scale climate variability across the Mediterranean region during proto-historic times (Mayewski et al., 2004; Piva et al., 2008; Nieto-Moreno et al., 2011; Drake, 2012).

#### 4.4. Zone 4: 4.5–2 m

##### 4.4.1. Description

Similar to the upper part of the underlying zone M5-3, this zone exhibits low concentration values (from 840 to 1160 grains/g), and an autochthonous association dominated by *Pinus* and herbaceous taxa (Fig. 5).

##### 4.4.2. Interpretation

With respect to the underlying zone 3, this pollen association indicates the development of a more open vegetation (grassland), with few oaks and Mediterranean trees. A similar vegetation cover has been widely reported from the west coasts of Italy during the last 2000 years (Di Rita and Magri, 2012).

#### 5. Highstand sedimentation patterns, fluvial dynamics and vegetation landscapes

The mid–late Holocene stratigraphic architecture, combined with the network of paleochannels identified through remote sensing, geomorphological and geophysical analyses, documents a multifaceted depositional history of the Pisa Plain. Based on a multi-proxy record, changes in sedimentation patterns and paleodrainage system are framed in the local environmental–climate conditions deduced from the pollen record of core M5 (Fig. 5 and Section 5).

##### 5.1. Pre-alluvial phase (Eneolithic age: ca. 5000–4000 cal yr BP)

If compared with the decelerating sea-level trend starting at ca. 7000 cal yr BP along the Italian coasts under highstand conditions (Lambeck et al., 2004, 2011), siltation of the wide lagoon basin originally developed in the Pisa area during the maximum marine transgression took place ca. 2000 years later (Fig. 3A–D). Around 5000 cal yr BP, at the beginning of the Eneolithic age (Fig. 3A–D and Table 1), the lagoon evolved into a vast marshland, crossed by distributary channels attributable to both Arno and Serchio rivers (Amorosi et al., 2013a). This phase was concomitant with a major change in vegetation cover (transition from pollen zones 1 to 2; Fig. 5). The replacement of mixed deciduous/evergreen oak forests by mixed woodlands and *Alnus* carrs with grasslands reflects the end of the Holocene climatic optimum (Fletcher and Sánchez Goñi, 2008; Combourieu Nebout et al., 2009) and the establishment of less humid conditions (Fig. 5). This long-term trend of increasing aridity/forest regression, extensively recorded across the West Mediterranean after 5000 cal yr BP (Jalut et al., 2000; Magny et al., 2002), reasonably promoted high sediment delivery, which, in turn, favored lagoon infilling and delta development.

The relationship between climatic aridification and coastal progradation appears to climax at the transition from deltaic to alluvial sedimentation. Indeed, alluvial plain development was preceded by a short-lived phase of pronounced forest reduction (AP/NAP ratio) and decline of drought-sensitive mountain trees, probably reflecting the arid episode of the well-known 4.2 ka event (Fig. 5).

## 5.2. Alluvial phase (Bronze age–Present: ca. last 4000 cal yr BP)

### 5.2.1. Bronze–Iron age (ca. 4000–2500 cal yr BP)

Following the characteristic mid–late Holocene progradation trend, shared by all major Mediterranean delta systems (Somoza et al., 1998; Bellotti et al., 2004; Aguzzi et al., 2005; Vella et al., 2005; Amorosi et al., 2008, 2013b; Milli et al., 2013), the marshlands emerged and abruptly turned into floodplain areas at the transition with the Bronze



age, around 3800 cal yr BP (Fig. 3A–D). The establishment of an alluvial plain subject to recurring flooding events is testified by poorly-drained floodplain conditions and by the widespread occurrence of thick, coarse-grained overbank successions (Fig. 3A–D). These depositional features along with the rapidly changing drainage configuration (Fig. 4A) point to a Bronze–Iron phase of intense fluvial activity, high runoff rates and floodplain sedimentation, reasonably promoted by a dense channel network (Fig. 4A) and the progressive reduction of forests (sparsely wooded grasslands of pollen zone 3; Fig. 5). A semicoeval phase of alluvial plain overflow has been inferred by Marra et al. (2013) for the Tiber Plain during the last 3500 cal yr BP. Consistent with our paleohydrographic reconstructions (Fig. 4A), Benvenuti et al. (2006) documented at the nearby Pisa San Rossore archeological site (Fig. 1) a pre-Roman channel-fill, truncated by Roman fluvial sands, and a genetically-related overbank succession, whose upper portion is dated to the Iron age.

However, two events of rapid channel incision and fill abruptly interrupted this phase of intense alluvial aggradation, as clearly documented by stratigraphic and ERT data (Figs. 3, 4C). The sudden occurrence of high-energy, erosional phases is also recorded by the two concomitant peaks in reworked pollen grains and lagoon-derived marine palynomorphs from the floodplain succession of core M5 (Fig. 5).

Across the study area, the first erosive phase produced a 4–5m-deep incision within the underlying lagoon–paludal succession (Figs. 3B, 4C). Subsurface stratigraphy and the available radiocarbon ages constrain chronologically this event to the Eneolithic–Bronze transition, between ca. 3800 and 3600 cal yr BP, i.e. shortly after alluvial plain development (Fig. 3).

The timing of the second incision-fill event is more accurately constrained by a series of radiocarbon ages available from the fluvial–channel succession recovered at core M7 (Fig. 3D). Fluvial incision

occurred at the Bronze–Iron transition, cutting the underlying lagoon–paludal–floodplain clays down to ~5–6 m (Fig. 3C, D). In less than 200 years the river channel was filled (Fig. 3D), and alluvial aggradation persisted up to the beginning of the Etruscan age (ca. 2500 cal yr BP). In conjunction with this high-energy fluvial event, the paleoArno River abruptly changed its position and for the first time shifted south of its modern course (Fig. 4A).

Interestingly, two short-lived (centennial-scale) climatic events of increased humidity are recorded within the Bronze–Iron floodplain succession of core M5 (Abies peaks 1 and 2; Fig. 5), at stratigraphic intervals correlative with the top-of-channel bodies formed during the rapid incision-fill phases (see Figs. 3D and 5).

The integration of stratigraphic, geomorphological, geophysical and palynological data documents good synchronicity of highstand sedimentation patterns, fluvial dynamics (aggradation/degradation ratio) and local climate changes, on a variety of time scales. In contrast, no direct (archeological) or indirect (palynological) evidence of strong human frequentation and impact on the Pisa Plain landscape has been recovered for the Bronze–Iron period, to date (Ribecai, 2011; Di Rita and Magri, 2012; Amorosi et al., 2013a).

#### 5.2.2. Etruscan age to Present (ca. 2500 cal yr BP–Present)

The beginning of the Etruscan age was characterized by the development of a complex alluvial setting under uninterrupted aggradational conditions. Low-lying backswamps, which became progressively inhabited, were formed north of the modern Arno River, between the proto-historic fluvial–channel systems (Amorosi et al., 2013a; Figs. 3, 4).

The transition to the Roman age (ca. 2000 cal yr BP) marked the early stage of the development of the modern Pisa Plain. This phase was characterized by the extensive growth of a well-drained alluvial plain, with widespread development of indurate horizons and grasslands (Figs. 3, 5). The natural tendency of both paleoArno and

paleoSerchio branches to change their courses was radically reduced by numerous waterworks (Martini et al., 2011), and wetland areas were partially reclaimed (Sarti et al., 2010). Since the Middle Ages onwards (ca. 1300–1400 cal yr BP; Table 1), an anthropogenic stratification occurred, revealing the progressive urbanization of the study area.

## 6. Discussion

The two events of channel incision and infill detected beneath the Pisa Plain at the transition between the Eneolithic–Bronze ages and the Bronze–Iron ages (~3800 cal yr BP and 2900–2800 cal yr BP; Figs. 3, 5) indicate the occurrence of high-frequency (centennial-scale), prominent changes in the aggradation/degradation ratio during the mid–late Holocene sea-level highstand.

In particular, increased fluvial activity:

- a) could be related to rapid (centennial-scale) climatic changes towards more humid conditions;
- b) could be the result of small amplitude relative sea-level changes (i.e. base-level changes);
- c) could represent the effect of human impact.

### 6.1. Climate

As widely documented in the literature (Ashley and Hamilton, 1993; Blum and Törnqvist, 2000; Lewis et al., 2001; Macklin et al., 2002; Straffin and Blum, 2002; Vandenberghe, 2003; Döll and Schmied, 2012), climate fluctuations at regional/sub-regional or global scale can induce significant changes in both discharge regime and sediment production and delivery to downstream locations. In the Pisa Plain, two (centennial-scale) climatic events of increased humidity occurred during the Eneolithic–Iron age, interrupting the long-term mid–late Holocene aridification trend (Abies peaks 1 and 2; Fig. 5). Radiocarbon and archeological dates (Fig. 3) allow to assign the two peaks of Abies to the Eneolithic–Bronze and Bronze–Iron transitions, around ~3800 cal yr BP and 2900–2800 cal yr BP, respectively (Fig. 5).

Within comparable time windows (Table 4), a number of multiproxy Mediterranean records provide evidence for two centennial-scale climatic events with similar characteristics (Nieto-Moreno et al., 2011; Roberts et al., 2011; Magny et al., 2012a,b; Fletcher and Zielhofer, 2013; Benito et al., 2015). The older one falls within the chronological interval of the well-known 4.2 ka event (Bond et al., 1997; Mayewski et al., 2004; Finné et al., 2011), which apparently shows a tripartite humidity oscillation between ~4300 and 3800 cal yr BP in the central-western Mediterranean area (Magny et al., 2009). In this regard, the first *Abies* peak recorded in core M5 might correspond to the wet phase closing the 4.2 ka event (Fig. 5).

Similarly, the youngest *Abies* peak recognized in core M5 (Fig. 5) resembles the new increase in humidity condition documented around 2800 cal yr BP from the western Mediterranean (Biserni and van Geel, 2005; Magny et al., 2007; Giraudi et al., 2011) and from west-central Europe (Magny, 2004) by high lake levels and pollen data.

As a whole, our data suggests i) the regional or supra-regional character of the two humidity peaks documented in this paper and ii) the close relationships between high-frequency climatic fluctuations and stratigraphic architecture, as shown by the strict correspondence between pollen signature and phases of fluvial erosion paralleled by an increase in reworked palynomorphs.

These data point towards the role played by climate fluctuations in triggering channel incision.

## 6.2. Relative sea-level changes

Relative sea-level (RSL) changes result from the interaction between global (eustatism) and local factors (i.e. hydrostasia, tectonic and sediment compaction), and produce a re-adjustment of the river longitudinal profile to the new base-level position. Specifically, fluvial incision can be triggered by RSL fall, although a direct, simple cause–effect relationship cannot be stated a priori (Schumm, 1993; Legarreta and Uliana, 1998).

Since the pioneering work of Pirazzoli (1976), the Holocene RSL history of the central Mediterranean basin has been investigated using different types of markers. The two most recent and reliable models (Spada and Stocchi, 2007; Lambeck et al., 2011) have been worked out cross-checking predictions with field data. Nevertheless, the two models misfit. Although the amount of available index points concerning the Holocene sea level in this area is remarkable and constantly increasing, there is still a certain amount of uncertainty on sealevel elevation even during the late Holocene (Morhange et al., 2001, 2006, 2013; Antonioli et al., 2007, 2009; Furlani et al., 2011; Primavera et al., 2011; Spampinato et al., 2011; Bini et al., 2012; Evelpidou et al., 2012; Amato et al., 2013).

Small-amplitude sea-level lowering along the Tyrrhenian coastline during the late Holocene has been hypothesized by Benvenuti et al. (2006) and Marra et al. (2013). However, clear evidence of protohistoric eustatic fall episodes has not been reported, to date. In contrast, all most detailed RSL predicted curves (Lambeck et al., 2004, 2011; Spada and Stocchi, 2007) match on a progressive rising trend since about 6000 cal yr BP. Moreover, the extensional tectonic context of the Pisa Plain, placed within the subsiding Viareggio Basin (Mariani and Prato, 1988; Argnani et al., 1997; Pascucci, 2005) and land subsidence induced by high compressible fine-grained deposits compaction (Rossi et al., 2011; Sarti et al., 2012) have enhanced this RSL rising trend through the addition of new accommodation space (Posamentier et al., 1988; Catuneanu, 2006; Hu and Plint, 2009).

Based on these data, there is currently no evidence of a link between RSL and the triggering of the two erosive processes. Conversely, the peculiar geotechnical features (high compressibility and plasticity) of the lagoon clays beneath the city of Pisa (Ministero dei Lavori Pubblici, 1971; Callisto and Calbresi, 1998; Sarti et al., 2012) could have enhanced to some degree the rate and the value of channel incisions, as documented by experimental data achieved in the Venice lagoon deposits

(Amos et al., 2010).

### 6.3. Human impact

An intensive human frequentation of the Pisa Plain area started off during the Iron–Etruscan transition (around 2500 cal yr BP), about three centuries later than the most recent proto-historic channel incision (Benvenuti et al., 2006; Mariotti Lippi et al., 2007; Bellini et al., 2009; Ribecai, 2011; Di Rita and Magri, 2012; Amorosi et al., 2013a). Only sporadic human settlements dated to the proto-historic period are documented on the surrounding highlands (Bagnone, 1982; Pasquinucci, 1994; Grifoni Cremonesi, 2006). In this respect, changes in land use patterns or any other type of human influence appear to be unrelated to the onset and/or amplification of the two events of fluvial incision.

### 7. Conclusions

A multi-proxy study of the mid–late Holocene deltaic–alluvial succession in the Pisa Plain reveals short-term fluvial evolution and changes in sedimentation patterns under relative sea-level highstand conditions (last ~7000 cal yr BP). The integration of high-resolution stratigraphic and paleohydrographic reconstructions with pollen data provides valued information about the relationships between fluvial dynamics and local paleoenvironmental–paleoclimate conditions.

The major outcomes of this study can be summarized as follows:

- (i) deltaic progradation took place with a long-term mid–late Holocene aridification. The transition to a genuine alluvial plain was immediately predated by a short-lived phase of pronounced forest reduction around 4200 cal yr BP;
- (ii) stratigraphic and paleohydrographic features reveal a Bronze–Iron age phase of high fluvial activity, increased runoff and floodplain sedimentation promoted by a dense channel network, involving Arno and Auser river courses, in an open vegetation landscape (sparsely wooded grasslands);

(iii) the proto-historic phase of intense alluvial aggradation was punctuated by two rapid events of enhanced fluvial incision that cut down to 10 m the underlying lagoonal substrate. Radiocarbon and archeological data constrain these events to the Eneolithic–Bronze age and Bronze–Iron age transitions (~3800 cal yr BP and 2900–2800 cal yr BP, respectively); (iii) the correlation between these events and two phases of increased humidity (Abies peaks 1 and 2) suggests that climate played a role in triggering channels incision;

(iv) relative sea-level changes did not played a significant role in the activation of fluvial incision, while the substrate nature (highly compressible lagoon clays) may have fostered the deepening of the channels;

(vi) mid–late Holocene (HST) coastal plain deposits formed in subsiding basin settings are excellent archive to elaborate highresolution depositional models, and may represent reliable past analogues on which to infer the potential response of modern environments to future climatic variations.

#### Acknowledgments

We thank the archeological staff of theMAPPA project for its support and suggestions. We are also grateful to Prof. Thierry Corrège and the reviewers for their useful comments.

#### References

- Aguzzi, M., Amorosi, A., Sarti, G., 2005. Stratigraphic architecture of Late Quaternary deposits in the lower Arno Plain (Tuscany, Italy). *Geol. Romana* 38, 1–10.
- Aguzzi, M., Amorosi, A., Colalongo, M.L., Ricci Lucchi, M., Rossi, V., Sarti, G., Vaiani, S.C., 2007. Late Quaternary climatic evolution of the Arno coastal plain (Western Tuscany, Italy) from subsurface data. *Sediment. Geol.* 202, 211–229.
- Alley, R.B., Marotzke, J., Nordhaus, W.D., Overpeck, J.T., Peteet, D.M., Pielke, R.A., Wallace, J.M., 2003. Abrupt climate change. *Science* 299 (5615), 2005–2010.

Amato, V., Aucelli, P.P.C., Ciampo, G., Cinque, A., Di Donato, V., Pappone, G., Petrosino, P., Romano, P., Roskopf, C.M., Russo Ermolli, E., 2013. Relative sea level changes and paleogeographical evolution of the southern Sele plain (Italy) during the Holocene. *Quat. Int.* 288, 112–128.

Amorosi, A., Milli, S., 2001. Late Quaternary depositional architecture of Po and Tevere river deltas (Italy) and worldwide comparison with coeval deltaic successions. *Sediment. Geol.* 144 (3), 357–375.

Amorosi, A., Dinelli, E., Rossi, V., Vaiani, S.C., Sacchetto, M., 2008. Late Quaternary palaeoenvironmental evolution of the Adriatic coastal plain and the onset of Po River Delta. *Palaeogeogr. Palaeoclimatol. Palaeoecol.* 268 (1–2), 80–90.

Amorosi, A., Ricci Lucchi, M., Rossi, V., Sarti, G., 2009. Climate change signature of smallscale parasequences from Lateglacial–Holocene transgressive deposits of the Arno valley fill. *Palaeogeogr. Palaeoclimatol. Palaeoecol.* 273, 142–152.

Amorosi, A., Rossi, V., Sarti, G., Mattei, R., 2013a. Coalescent valley fills from the late Quaternary record of Tuscany (Italy). *Quat. Int.* 288, 129–138.

Amorosi, A., Bini, M., Giacomelli, S., Pappalardo, M., Ribecai, C., Rossi, V., Sammartino, I., Sarti, G., 2013b. Middle to late Holocene environmental evolution of the Pisa coastal plain (Tuscany, Italy) and early human settlements. *Quat. Int.* 303, 93–106.

Amos, C.L., Umgieser, G., Ferrarin, C., Thompson, C.E.L., Whitehouse, R.J.S., Sutherland, T.F., Bergamasco, A., 2010. The erosion rates of cohesive sediments in Venice lagoon. *Cont. Shelf Res.* 30, 859–870.

Antonioli, F., Anzidei, M., Lambeck, K., Auriemma, R., Gaddi, D., Furlani, S., Orrù, P., Solinas, E., Gaspari, A., Karinja, S., Kovačić, V., Surace, L., 2007. Sea-level change during the Holocene in Sardinia and in the northeastern Adriatic (central Mediterranean Sea) from archaeological and geomorphological data. *Quat. Sci. Rev.* 26 (19–21), 2463–2486.

Antonioli, F., Ferranti, L., Fontana, A., Amorosi, A., Bondesan, A., Braitenberg, C., Dutton, A., Fontolan, G., Furlani, S., Lambeck, K., Mastronuzzi, G., Monaco, C., Spada, G., Stocchi, P., 2009. Holocene relative sea-level changes and vertical movements along the Italian and Istrian coastlines. *Quat. Int.* 206 (1–2), 102–133.

Argnani, A., Bernini, M., Di Dio, G.M., Papani, G., Rogledi, S., 1997. Stratigraphic record of crustal scale tectonics in the Quaternary of the Northern Apennines (Italy). II



Quaderno 10, 595–602.

Ashley, G.M., Hamilton, T.D., 1993. Fluvial response to late Quaternary climatic fluctuations, central Kobuk Valley, northwestern Alaska. *J. Sediment. Res.* 63 (5).

Bagnone, D., 1982. L'insediamento neolitico e dell'inizio dell'età dei metalli di Poggio di Mezzo (San Rossore, Pisa). *Atti Soc. Toscana Sci. Nat. Resid. Pisa Mem. Ser. A* 89, 61–82.

Bar-Matthews, M., Ayalon, A., 2011. Mid-Holocene climate variations revealed by high-resolution speleothem records from Soreq Cave, Israel and their correlation with cultural changes. *The Holocene* 21 (1), 163–171.

Bellini, C., Mariotti Lippi, M., Montanari, C., 2009. The Holocene landscape history of the NW Italian coasts. *The Holocene* 19 (8), 1161–1172.

Bellotti, P., Caputo, C., Davoli, L., Evangelista, S., Garzanti, E., Pugliese, F., Valeri, P., 2004. Morpho-sedimentary characteristics and Holocene evolution of the emergent part of the Ombrone River delta (southern Tuscany). *Geomorphology* 61 (1), 71–90.

Benito, G., Sopeña, A., Sánchez-Moya, Y., Machado, M.J., Pérez-González, A., 2003. Palaeoflood record of the Tagus River (Central Spain) during the Late Pleistocene and Holocene. *Quat. Sci. Rev.* 22 (15–17), 1737–1756.

Benito, G., Macklin, M.G., Zielhofer, C., Jones, A.F., Machado, M.J., 2014. Holocene flooding and climate change in the Mediterranean. *Catena* <http://dx.doi.org/10.1016/j.catena.2014.11.014>.

Benito, G., Macklin, M.G., Cohen, K.M., Herget, J., 2015. Past hydrological extreme events in a changing climate. *Catena* <http://dx.doi.org/10.1016/j.catena.2014.12.001>.

Benvenuti, M., Mariotti Lippi, M., Pallecchi, P., Sagri, M., 2006. Late-Holocene catastrophic floods in the terminal Arno River (Pisa, Central Italy) from the history of a Roman riverine harbor. *The Holocene* 16 (6), 863–876.

Bini, M., Brückner, H., Chelli, A., Pappalardo, M., Da Prato, S., Gervasini, L., 2012. Palaeogeographies of the Magra Valley coastal plain to constrain the location of the Roman harbour of Lunae (NW Italy). *Palaeogeogr. Palaeoclimatol. Palaeoecol.* 337, 37–51.

Biserni, G., Van Geel, B., 2005. Reconstruction of Holocene palaeoenvironment and sedimentation history of the Ombrone alluvial plain (South Tuscany, Italy). *Rev. Palaeobot. Palynol.* 136 (1), 16–28.

- Bisson, M., Bini, M., 2012. A multidisciplinary approach to reveal palaeohydrographic features: the case study of Luna archaeological site surroundings. *Int. J. Geogr. Inf. Sci.* 26, 327–343.
- Blum, M.D., Törnqvist, T.E., 2000. Fluvial responses to climate and sea-level change: a review and look forward. *Sedimentology* 47 (1), 2–48.
- Bond, G., Showers, W., Cheseby, M., Lotti, R., Almasi, P., DeMenocal, P., Priore, P., Cullen, H., Hajdas, I., Bonani, G., 1997. A pervasive millennial-scale cycle in North Atlantic Holocene and glacial climates. *Science* 278 (5341), 1257–1266.
- Bond, G., Kromer, B., Beer, J., Muscheler, R., Evans, M.N., Showers, W., Hoffmann, S., Lotti-Bond, R., Hajdas, I., Bonani, G., 2001. Persistent solar influence on North Atlantic climate during the Holocene. *Science* 294 (5549), 2130–2136.
- Bruni, S., Cosci, M., 2003. *Alpheae veterem contemptlor originis urbem, quam cingunt geminis Arnus et Ausur aquis. Il paesaggio di Pisa etrusca e romana: materiali e problemi.* In: Bruni, S. (Ed.), *Il porto urbano di Pisa. La fase etrusca. Il contesto e il relitto ellenistico*, Pisa, pp. 29–43.
- Callisto, L., Calbresi, G., 1998. Mechanical behavior of natural soft clay. *Geotechnique* 48, 495–513.
- Catuneanu, O., 2006. *Principles of Sequence Stratigraphy*. Elsevier, Amsterdam, p. 375.
- Catuneanu, O., Abreu, V., Bhattacharya, J.P., Blum, M.D., Dalrymple, R.W., Eriksson, P.G., Fielding, C.R., Fisher, W.L., Galloway, W.E., Gibling, M.R., Giles, K.A., Holbrook, J.M., Jordan, R., Kendall, C.G.St.C., Macurda, B., Martinsen, O.J., Miall, A.D., Neal, J.E., Nummedal, D., Pomar, L., Posamentier, H.W., Pratt, B.R., Sarg, J.F., Shanley, K.W., Steel, R.J., Strasser, A., Tucker, M.E., Winker, C., 2009. Towards the standardization of sequence stratigraphy. *Earth Sci. Rev.* 92 (1), 1–33.
- Combourieu Nebout, N., Peyron, O., Dormoy, I., Desprat, S., Beaudouin, C., Kotthoff, U., Marret, F., 2009. Rapid climatic variability in the west Mediterranean during the last 25,000 years from high-resolution pollen. *Clim. Past* 5 (3), 503–521.
- Di Pasquale, G., Allevato, E., Cocchiara, A., Moser, D., Pacciarelli, M., Saracino, A., 2014. Late Holocene persistence of *Abies alba* in low–mid altitude deciduous forests of central and southern Italy: new perspectives from charcoal data. *J. Veg. Sci.* 25 (5), 1299–1310.

- Di Rita, F., Magri, D., 2012. An overview of the Holocene vegetation history from the central Mediterranean coasts. *J. Mediterr. Earth Sci.* 4, 35–52.
- Di Rita, F., Celant, A., Magri, D., 2010. Holocene environmental instability in the wetland north of the Tiber delta (Rome, Italy): sea–lake–man interactions. *J. Paleolimnol.* 44 (1), 51–67.
- Döll, P., Schmied, H.M., 2012. How is the impact of climate change on river flow regimes related to the impact on mean annual runoff? A global-scale analysis. *Environ. Res. Lett.* 7 (1), 014037.
- Drake, B.L., 2012. The influence of climatic change on the Late Bronze Age Collapse and the Greek Dark Ages. *J. Archaeol. Sci.* 39, 1862–1870.
- Drescher-Schneider, R., De Beaulieu, J.-L., Magny, M., Walter-Simonnet, A.-V., Bossuet, G., Millet, L., Brugiapaglia, E., Drescher, A., 2007. Vegetation history, climate and human impact over the last 15,000 years at Lago dell'Accesa (Tuscany, Central Italy). *Veg. Hist. Archaeobot.* 16 (4), 279–299.
- Evelpidou, N., Pirazzoli, P., Vassilopoulos, A., Spada, G., Ruggieri, G., Tomasin, A., 2012. Late Holocene sea level reconstructions based on observations of roman fish tanks, Tyrrhenian coast of Italy. *Geoarchaeology* 27 (3), 259–277.
- Fægri, K., Iversen, J., 1989. In: Fægri, K., Kaland, P., Krzywinski, K. (Eds.), *Textbook of Pollen Analysis*, fourth ed. Wiley, Chichester.
- Fanget, A.S., Berné, S., Jouet, G., Bassetti, M.A., Dennielou, B., Maillet, G.M., Tondut, M., 2014. Impact of relative sea level and rapid climate changes on the architecture and lithofacies of the Holocene Rhone subaqueous delta (Western Mediterranean Sea). *Sediment. Geol.* 305, 35–53.
- Finné, M., Holmgren, K., Sundqvist, H.S., Weiberg, E., Lindblom, M., 2011. Climate in the eastern Mediterranean, and adjacent regions, during the past 6000 years. A review. *J. Archaeol. Sci.* 38 (12), 3153–3173.
- Fletcher, W.J., Sánchez Goñi, M.F., 2008. Orbital- and sub-orbital-scale climate impacts on vegetation of the western Mediterranean basin over the last 48,000 yr. *Quat. Res.* 70, 451–464.
- Fletcher, W.J., Zielhofer, C., 2013. Fragility of Western Mediterranean landscapes during Holocene rapid climate changes. *Catena* 103, 16–29.
- Furlani, S., Biolchi, S., Cucchi, F., Antonioli, F., Buseti, M., Melis, R., 2011. Tectonic effects on

Late Holocene sea level changes in the Gulf of Trieste (NE Adriatic Sea, Italy). *Quat. Int.* 232 (1–2), 144–157.

Giraudi, C., Magny, M., Zanchetta, G., Drysdale, R.N., 2011. The Holocene climatic evolution of Mediterranean Italy: a review of the continental geological data. *The Holocene* 21 (1), 105–115.

Grifoni Cremonesi, R., 2006. Il neolitico e l'età dei metalli in Toscana: sviluppi culturali e strategie insediative. In: Peruzzi, A. (Ed.), *Pianeta Galileo*, pp. 199–211 (Firenze).

Helama, S., Fauria, M.M., Mielikäinen, K., Timonen, M., Eronen, M., 2010. Sub-Milankovitch solar forcing of past climates: mid and late Holocene perspectives. *Geol. Soc. Am. Bull.* 122 (11–12), 1981–1988.

Hemming, S.R., 2004. Heinrich events: massive late Pleistocene detritus layers of the North Atlantic and their global climate imprint. *Rev. Geophys.* 42 (1), RG1005.  
<http://dx.doi.org/10.1029/2003RG000128>.

Hu, Y.G., Plint, A.G., 2009. An allostratigraphic correlation of a mudstone-dominated, syntectonic wedge: the Puskwaskau Formation (Santonian–Campanian) in outcrop and subsurface, Western Canada Foreland Basin. *Bull. Can. Petrol. Geol.* 57 (1), 1–33.

Jalut, G., Esteban Amat, A., Bonnet, L., Gauquelin, T., Fontugne, M., 2000. Holocene climatic changes in the Western Mediterranean, from southeast France to south-east Spain. *Palaeogeogr. Palaeoclimatol. Palaeoecol.* 160 (3–4), 255–290.

Jones, A.F., Macklin, M.G., Lewin, J., 2010. Flood series data for the later Holocene: available approaches, potential and limitations from UK alluvial sediments. *The Holocene* 20, 1123–1135.

Lambeck, K., Antonioli, F., Purcell, A., Silenzi, S., 2004. Sea-level change along the Italian coast for the past 10,000 yr. *Quat. Sci. Rev.* 23 (14), 1567–1598.

Lambeck, K., Antonioli, F., Anzidei, M., Ferranti, L., Leoni, G., Scicchitano, G., Silenzi, S., 2011. Sea level change along the Italian coast during the Holocene and projections for the future. *Quat. Int.* 232 (1–2), 250–257.

Legarreta, L., Uliana, M.A., 1998. Anatomy of hinterland depositional sequences: Upper Cretaceous fluvial strata, Neuquen Basin, West-Central Argentina. In: Shanley, K.W., McCabe, P.J. (Eds.), *Relative Role of Eustasy, Climate, and Tectonism in Continental Rocks*. *Spec. Publ. Soc. Econ. Paleont. Miner.* 59, pp. 83–92.

Lewin, J., Macklin, M.G., Johnstone, E., 2005. Interpreting alluvial archives: sedimentological

factors in the British Holocene fluvial record. *Quat. Sci. Rev.* 24, 1873–1889.

Lewis, S.G., Maddy, D., Scaife, R.G., 2001. The fluvial system response to abrupt climate change during the last cold stage: the Upper Pleistocene River Thames fluvial succession at Ashton Keynes, UK. *Glob. Planet. Chang.* 28 (1), 341–359.

Macklin, M.G., Lewin, J., 2003. River sediments, great floods and centennial-scale Holocene climate change. *J. Quat. Sci.* 18 (2), 101–105.

Macklin, M.G., Fuller, I.C., Lewin, J., Maas, G.S., Passmore, D.G., Rose, J., Woodward, J.C., Black, S., Hamblin, R.H.B., Rowan, J.S., 2002. Correlation of fluvial sequences in the Mediterranean basin over the last 200 ka and their relationship to climate change. *Quat. Sci. Rev.* 21, 1633–1641.

Macklin, M.G., Benito, G., Gregory, K.J., Johnstone, E., Lewin, J., Michczyńska, D.J., Soja, R., Starkel, L., Thorndycraft, V.R., 2006. Past hydrological events reflected in the Holocene fluvial record of Europe. *Catena* 66 (1), 145–154.

Macklin, M.G., Lewin, J., Woodward, J.C., 2012. The fluvial record of climate change. *Philosophical Transactions of the Royal Society A: mathematical. Phys. Eng. Sci.* 370 (1966), 2143–2172.

Maddy, D., Bridgland, D., Westaway, R., 2001. Uplift-driven valley incision and climate-controlled river terrace development in the Thames Valley, UK. *Quat. Int.* 79 (1), 23–36.

Magny, M., 2004. Holocene climatic variability as reflected by mid-European lake-level fluctuations, and its probable impact on prehistoric human settlements. *Quat. Int.* 113, 65–79.

Magny, M., Miramont, C., Sivan, O., 2002. Assessment of the impact of climate and anthropogenic factors on Holocene Mediterranean vegetation in Europe on the basis of palaeohydrological records. *Palaeogeogr. Palaeoclimatol. Palaeoecol.* 186, 47–59.

Magny, M., de Beaulieu, J.-L., Bégeot, C., Heiri, O., Millet, L., Peyron, O., Walter-Simonnet, A.V., 2007. Holocene climate changes in the central Mediterranean as recorded by lake-level fluctuations at Lake Accesa (Tuscany, Italy). *Quat. Sci. Rev.* 26 (13), 1736–1758.

Magny, M., Vannièrè, B., Zanchetta, G., Fouache, E., Touchais, G., Petrika, L., Coussot, C., Walter-Simonnet, A.-V., Arnaud, F., 2009. Possible complexity of the climatic event around 4300–3800 cal. BP in the central and western Mediterranean. *The Holocene* 19 (6), 823–833.

- Magny, M., Peyron, O., Sadori, L., Ortu, E., Zanchetta, G., Vanni re, B., Tinner, W., 2012a. Contrasting patterns of precipitation seasonality during the Holocene in the south and north-central Mediterranean. *J. Quat. Sci.* 27 (3), 290–296.
- Magny, M., Arnaud, F., Billaud, Y., Marguet, A., 2012b. Lake-level fluctuations at Lake Bourget (eastern France) around 4500–3500 cal. a BP and their palaeoclimatic and archaeological implications. *J. Quat. Sci.* 27 (5), 494–502.
- Magri, D., 2007. Advances in Italian palynological studies: late Pleistocene and Holocene records. *GFF* 129 (4), 337–344.
- Malinverno, A., Ryan, W.B., 1986. Extension in the Tyrrhenian Sea and shortening in the Apennines as result of arc migration driven by sinking of the lithosphere. *Tectonics* 5 (2), 227–245.
- Mariani, M., Prato, R., 1988. I bacini neogenici costieri del margine tirrenico: approccio sismico stratigrafico. *Geol. Ital. Mem.* 41, 519–531.
- Mariotti Lippi, M.M., Bellini, C., Trinci, C., Benvenuti, M., Pallecchi, P., Sagri, M., 2007. Pollen analysis of the ship site of Pisa San Rossore, Tuscany, Italy: the implications for catastrophic hydrological events and climatic change during the late Holocene. *Veg. Hist. Archaeobot.* 16 (6), 453–465.
- Marra, F., Bozzano, F., Cinti, F.R., 2013. Chronostratigraphic and lithologic features of the Tiber River sediments (Rome, Italy): implications on the post-glacial sea-level rise and Holocene climate. *Glob. Planet. Chang.* 107, 157–176.
- Martini, I.P., Sagri, M., 1993. Tectono-sedimentary characteristics of Late Miocene–Quaternary extensional basins of the Northern Apennines, Italy. *Earth Sci. Rev.* 34 (3), 197–233.
- Martini, I.P., Sarti, G., Pallecchi, P., Costantini, A., 2011. Landscape influences on the development of the Medieval–Early Renaissance city-states of Pisa, Florence, and Siena, Italy. *Landscapes and Societies* (pp. 203–221). Springer, Netherlands, p. 467.
- Mayewski, P.A., Rohling, E.E., Stager, J.C., Karlen, W., Maasch, K.A., Meeker, L.D., Meyerson, E.A., Gasse, F., van Kreveld, S., Holmgren, K., Lee-Thorp, J., Rosqvist, G., Rack, F., Staubwasser, M., Schneider, R.R., Steig, E.J., 2004. Holocene climate variability. *Quat. Res.* 62, 243–255.
- Miall, A.D., 1996. *The Geology of Fluvial Deposits*. Springer-Verlag, p. 582.
- Milli, S., D'Ambrogi, C., Bellotti, P., Calderoni, G., Carboni, M.G., Celant, A., Di Bella, L., Di Rita, F., Frezza, V., Magri, D., Pichezzi, R.M., Ricci, V., 2013. The transition from

wave-dominated estuary to wave-dominated delta: the Late Quaternary stratigraphic architecture of Tiber River deltaic succession (Italy). *Sediment. Geol.* 284–285, 159–180.

Ministero dei Lavori Pubblici, 1971. Ricerche e studi sulla Torre pendente di Pisa e i fenomeni connessi alle condizioni d'ambiente. Istituto Geografico Militare, Firenze (I, II, III).

Morhange, C., Laborel, J., Hesnard, A., 2001. Changes of relative sea level during the past 5000 years in the ancient harbor of Marseilles, Southern France. *Palaeogeogr. Palaeoclimatol. Palaeoecol.* 166 (3–4), 319–329.

Morhange, C., Pirazzoli, P.A., Marriner, N., Montaggioni, L.F., Nammour, T., 2006. Late Holocene relative sea-level changes in Lebanon, Eastern Mediterranean. *Mar. Geol.* 230 (1–2), 99–114.

Morhange, C., Marriner, N., Excoffon, P., Bonnet, S., Flaux, C., Zibrowius, H., Goiran, J.P., Amouri, M.E., 2013. Relative sea-level changes during Roman Times in the Northwest Mediterranean: the 1st century A.D. Fish tank of Forum Julii, Fréjus, France. *Geoarchaeology* 28 (4), 363–372.

Nieto-Moreno, V., Martínez-Ruiz, F., Giral, S., Jiménez-Espejo, F., Gallego-Torres, D., Rodrigo-Gámiz, M., García-Orellana, J., Ortega-Huertas, M., De Lange, G.J., 2011. Tracking climate variability in the western Mediterranean during the Late Holocene: a multiproxy approach. *Clim. Past* 7 (4), 1395–1414.

Pascucci, V., 2005. Neogene evolution of the Viareggio Basin, northern Tuscany (Italy). *Geol. Acta* 4, 123–138.

Pasquinucci, 1994. Il popolamento dall'età del Ferro al Tardo Antico. In: Mazzanti, R. (Ed.), *La pianura di Pisa ed i rilievi contermini*.

Patacca, E., Sartori, P., Scandone, P., 1993. Tyrrhenian basin and Apennines. Kinematic evolution and related dynamic constraints. In: Boschi, E., Mantovani, E., Morelli, A. (Eds.), *Recent Evolution and Seismicity of the Mediterranean Region*. Kluwer Academic Publishers, Dordrecht, Netherlands, pp. 161–171.

Pirazzoli, P.A., 1976. Sea level variations in the northwest Mediterranean during Roman times. *Science* 194 (4264), 519–521.

Piva, A., Asioli, A., Trincardi, F., Schneider, R.R., Vigliotti, L., 2008. Late-Holocene climate variability in the Adriatic sea (Central Mediterranean). *The Holocene* 18 (1),

153–167.

Posamentier, H.W., Jervey, M.T., Vail, P.R., 1988. Eustatic controls on clastic deposition I — conceptual framework. In: Wilgus, C.K., Hastings, B.S., C. G. St, Kendall, C., Posamentier, H.W., Ross, C.A., Van Wagoner, J.C. (Eds.), *Sea Level Change: An Integrated Approach*. SEPM Special Publication 42, pp. 110–124.

Pranzini, E., 2001. Updrift river mouth migration on cusped deltas: two examples from the coast of Tuscany (Italy). *Geomorphology* 38 (1–2), 125–132.

Primavera, M., Simone, O., Fiorentino, G., Caldara, M., 2011. The palaeoenvironmental study of the Alimini Piccolo lake enables a reconstruction of Holocene sea-level changes in southeast Italy. *The Holocene* 21 (4), 553–563.

Reille, M., 1992–98. *Pollen et spores d'Europe et d'Afrique du Nord*. Laboratoire de botanique historique et palynologie, Marseille.

Reimer, P.J., Baillie, M.G.L., Bard, E., Bayliss, A., Beck, J.W., Blackwell, P.G., Bronk Ramsey, C., Buck, C.E., Burr, G.S., Edwards, R.L., Friedrich, M., Grootes, P.M., Guilderson, T.P., Hajdas, I., Heaton, T.J., Hogg, A.G., Hughen, K.A., Kaiser, K.F., Kromer, B., McCormac, F.G., Manning, S.W., Reimer, R.W., Richards, D.A., Southon, J.R., Talamo, S., Turney, C.S.M., van der Plicht, J., Weyhenmeyer, C.E., 2009. INTCAL 09 and MARINE09 radiocarbon age calibration curves, 0, 50,000 years Cal BP. *Radiocarbon* 51, 1111–1150.

Ribecai, C., 2011. Synthesis of Late Quaternary palynological studies in the Arno coastal plain and surroundings: toward a comprehensive Late Quaternary palaeovegetational history. *Atti Soc. Toscana Sci. Nat. Mem. Ser. A* 116, 163–170.

Ricci Lucchi, M., 2008. Vegetation dynamics during the last interglacialeglacial cycle in the Arno coastal plain (Tuscany, western Italy): location of a new tree refuge. *Quat. Sci. Rev.* 27, 2456–2466.

Roberts, N., Eastwood, W.J., Kuzucuo lu, C., Fiorentino, G., Caracuta, V., 2011. Climatic, vegetation and cultural change in the eastern Mediterranean during the mid-Holocene environmental transition. *The Holocene* 21 (1), 147–162.

Rossi, V., Amorosi, A., Sarti, G., Potenza, M., 2011. Influence of inherited topography on the Holocene sedimentary evolution of coastal systems: an example from Arno coastal plain (Tuscany, Italy). *Geomorphology* 135 (1), 117–128.

Rossi, V., Amorosi, A., Sarti, G., Romagnoli, R., 2012. New stratigraphic evidence for the mid-late Holocene fluvial evolution of the Arno coastal plain (Tuscany, Italy)



[Données stratigraphiques nouvelles concernant l'évolution fluviale de la plaine côtière de Arno (Toscane, Italie) à l'Holocène moyen-supérieur]. *Geomorphol. Relief Process. Environ.* 2, 201–214.

Sadori, L., Jahns, S., Peyron, O., 2011. Mid-Holocene vegetation history of the central Mediterranean. *The Holocene* 21 (1), 117–129.

Sarti, G., Bini, M., Serena, G., 2010. The growth and the decline of Pisa (Tuscany, Italy) up to the Middle Ages: correlations with landscape and geology. In: geological setting and urban development of selected Italian towns up to the Middle Ages and legacies of ancient problems throughout the ages. *Il Quaderno dell'Ostetrica Ital. J. Quat. Sci.* 23 (2bis), 311–322.

Sarti, G., Rossi, V., Amorosi, A., 2012. Influence of Holocene stratigraphic architecture on ground surface settlements: a case study from the City of Pisa (Tuscany, Italy). *Sediment. Geol.* 281, 75–87.

Schumm, S.A., 1993. River response to base level change: implications for sequence stratigraphy. *J. Geol.* 101, 279–294.

Somoza, L., Barnolas, A., Arasa, A., Maestro, A., Rees, J.G., Hernández-Molina, F.J., 1998. Architectural stacking patterns of the Ebro delta controlled by Holocene highfrequency eustatic fluctuations, delta-lobe switching and subsidence processes. *Sediment. Geol.* 117 (1), 11–32.

Spada, G., Stocchi, P., 2007. SELEN: a Fortran 90 program for solving the “sea-level equation”. *Comput. Geosci.* 33 (4), 538–562.

Spampinato, C.R., Costa, B., Di Stefano, A., Monaco, C., Scicchitano, G., 2011. The contribution of tectonics to relative sea-level change during the Holocene in coastal southeastern Sicily: new data from boreholes. *Quat. Int.* 232 (1–2), 214–227.

Stanley, D.J., Warne, A.G., 1994. Worldwide initiation of Holocenemarine deltas by deceleration of sea-level rise. *Science* 265 (5169), 228–231.

Starkel, L., 1983. The reflection of hydrologic changes in the fluvial environment of the temperate zone during the last 15,000 years. *Background to Palaeohydrology* pp. 213–235.

Starkel, L., 2000. Heavy Rains and Floods in Europe During Last Millennium. *Reconstructions of Climate and Its Modeling, Prace geograficzne, 107.* Institute of Geography of the Jagiellonian University, Cracow, pp. 55–62.

Starkel, L., Soja, R., Michczyńska, D.J., 2006. Past hydrological events reflected in Holocene

history of Polish rivers. *Catena* 66 (1), 24–33.

Steffensen, J.P., Andersen, K.K., Bigler, M., Clausen, H.B., Dahl-Jensen, D., Fischer, H., Goto-Azuma, K., Hansson, M., Johnsen, S.J., Jouzel, J., Masson-Delmotte, V., Popp, T., Rasmussen, S.O., Röthlisberger, R., Ruth, U., Stauffer, B., Siggaard-Andersen, M.L., Sveinbjörnsdóttir, Á.E., Svensson, A., White, J.W.C., 2008. High-resolution Greenland ice core data show abrupt climate change happens in few years. *Science* 321 (5889), 680–684.

Straffin, E.C., Blum, M.D., 2002. Holocene fluvial response to climate change and human activities; Burgundy, France. *Neth. J. Geosci. Geol. Mijnb* 81 (3), 417–430.

Thorndycraft, V.R., Benito, G., 2006. Late Holocene fluvial chronology of Spain: the role of climatic variability and human impact. *Catena* 66 (1), 34–41.

Tinner, W., Lotter, A.F., 2006. Holocene expansions of *Fagus sylvatica* and *Abies alba* in Central Europe: where are we after eight decades of debate? *Quat. Sci. Rev.* 25 (5–6), 526–549.

Tinner, W., Colombaroli, D., Heiri, O., Henne, P.D., Steinacher, M., Untenecker, J., Vescovi, E., Allen, J.R.M., Carraro, G., Conedera, M., Joos, F., Lotter, A.F., Luterbacher, J., Samartin, S., Valsecchi, V., 2013. The past ecology of *Abies alba* provides new perspectives on future responses of silver fir forests to global warming. *Ecol. Monogr.* 83 (4), 419–439.

Traverse, A., 1988. Plant evolution dances to a different beat: plant and animal evolutionary mechanisms compared. *Hist. Biol.* 1 (4), 277–301.

Turner, F., Tolkdorf, J.F., Viehberg, F., Schwalb, A., Kaiser, K., Bittmann, F., von Bramann, U., Pott, R., Staesche, U., Breest, K., Veil, S., 2013. Lateglacial/early Holocene fluvial reactions of the Jeezel River (Elbe valley, northern Germany) to abrupt climatic and environmental changes. *Quat. Sci. Rev.* 60, 91–109.

Vandenberghe, J., 2003. Climate forcing of fluvial system development: an evolution of ideas. *Quat. Sci. Rev.* 22 (20), 2053–2060.

Vella, C., Fleury, T.J., Raccasi, G., Provansal, M., Sabatier, F., Bourcier, M., 2005. Evolution of the Rhône delta plain in the Holocene. *Mar. Geol.* 222, 235–265.

Wanner, H., Beer Wanner, H., Beer, J., Bütikofer, J., Crowley, T.J., Cubasch, U., Flückiger, J., Gooße, H., Grosjean, M., Joos, F., Kaplan, J.O., Küttel, M., Müller, S.A., Prentice, I.C., Solomina, O., Stocker, T.F., Tarasov, P., Wagner, M., Widmann, M., 2008. Mid- to

Late Holocene climate change: an overview. *Quat. Sci. Rev.* 27 (19), 1791–1828.

Zanchetta, G., Bini, M., Cremaschi, M., Magny, M., Sadori, L., 2013. The transition from natural to anthropogenic-dominated environmental change in Italy and the surrounding regions since the Neolithic: an introduction. *Quat. Int.* 303, 1–9.

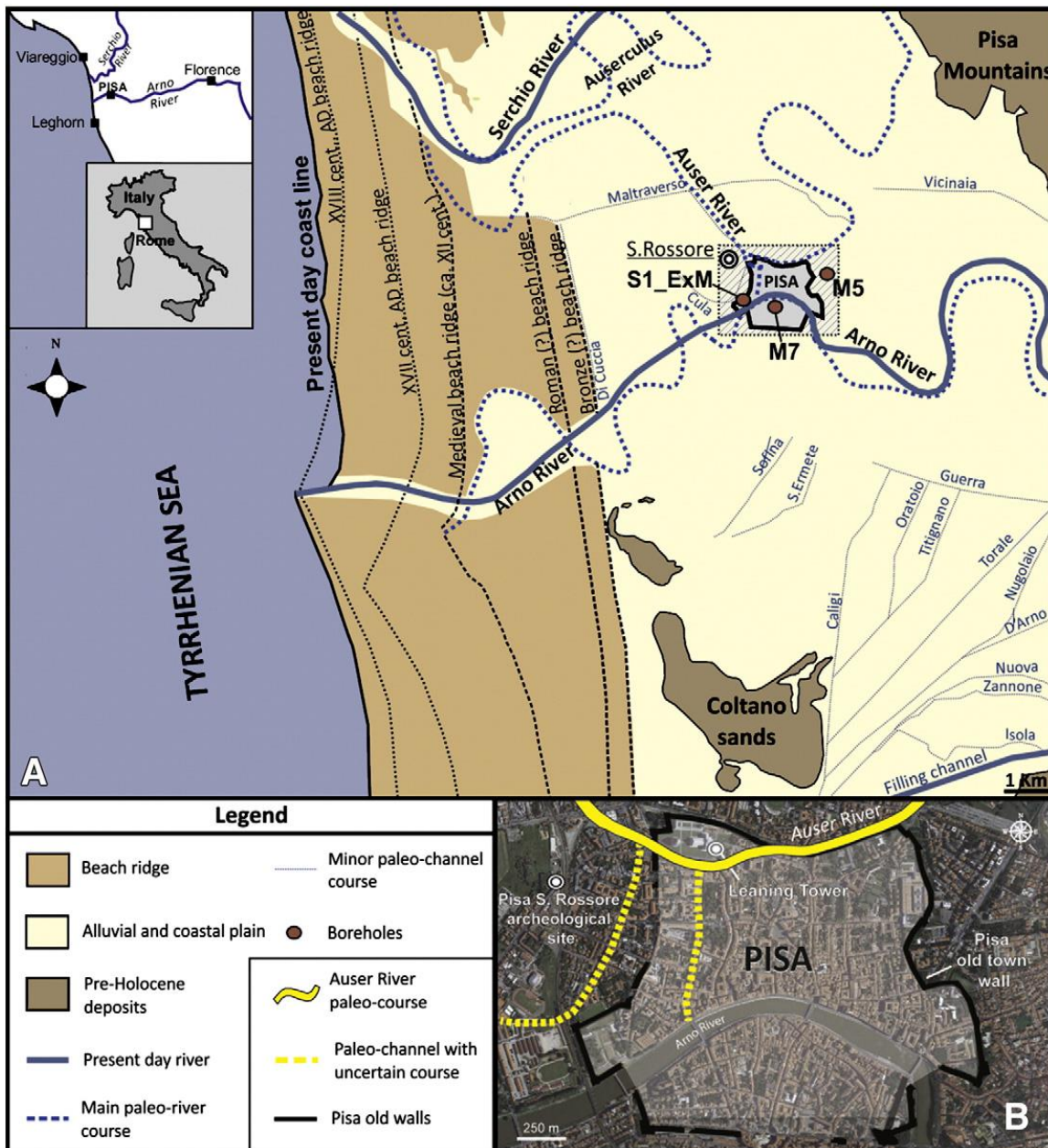


Fig. 1. A) Geological sketch map of the Pisa Plain with indication of the outcropping, juxtaposed coastal beach ridges and the Auser paleo-course hypothesized by Strabo (partially modified from Pranzini, 2001 and Sarti et al., 2010). The location of cores mentioned in text is also reported. B) Close-up of the study area corresponding to the Pisa urban and suburban zones. The Medieval city walls are shown with a bold line. The Auser paleo-course is also reported along with the location of the archaeological site of Pisa S. Rossore.



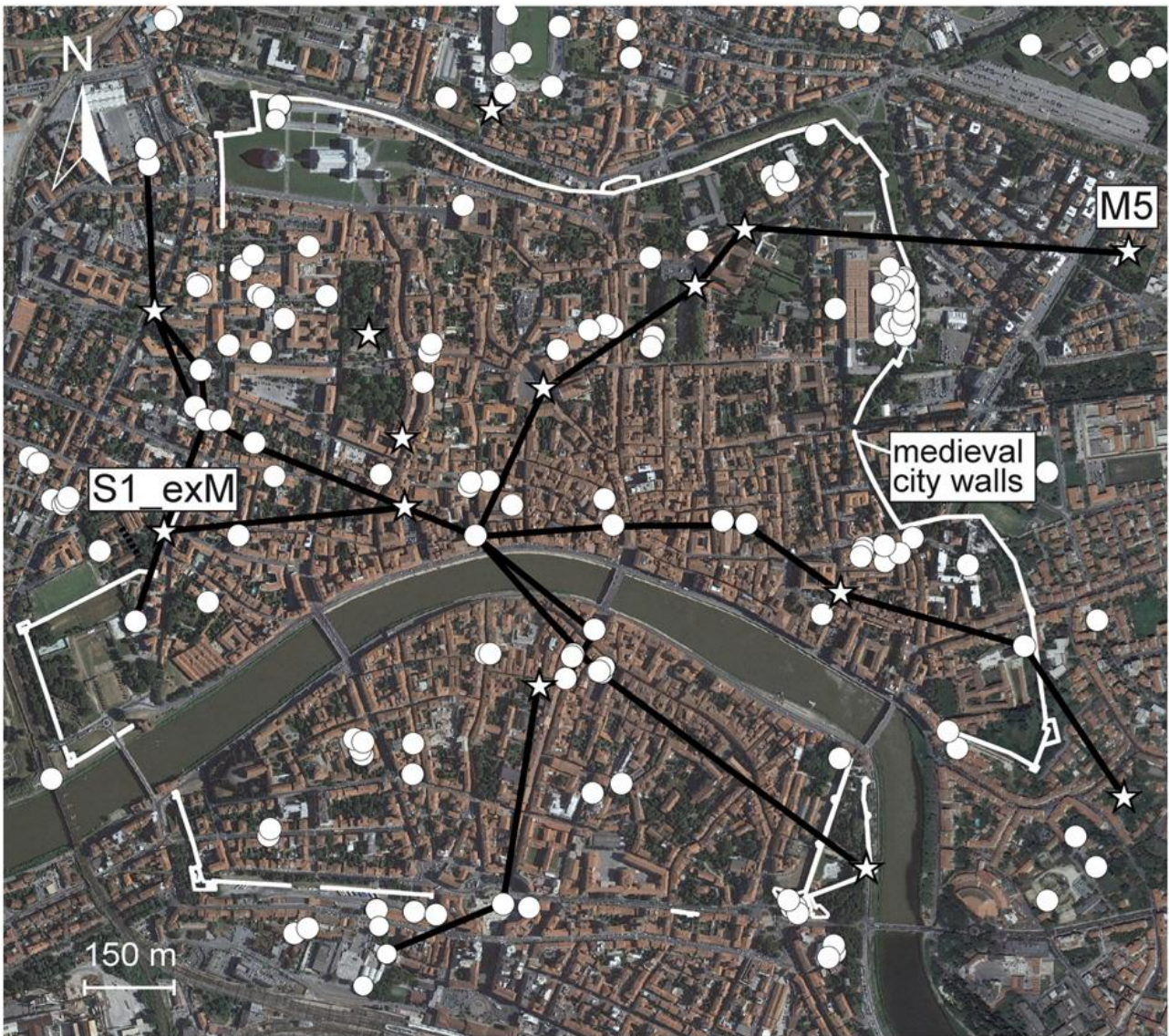


Fig. 2. Locationmap of the study area reporting the georeferenced subsurface dataset used for thiswork (from Amorosi et al., 2013b). The reference MAPPAs cores are shown by white stars. The location of cores M5 and S1\_exM, selected for palynological analysis and ERT calibration respectively, is highlighted. The bold lines and the dotted line indicate the cross-sections reported in Fig. 3 and the ERT profile of Fig. 4, respectively.

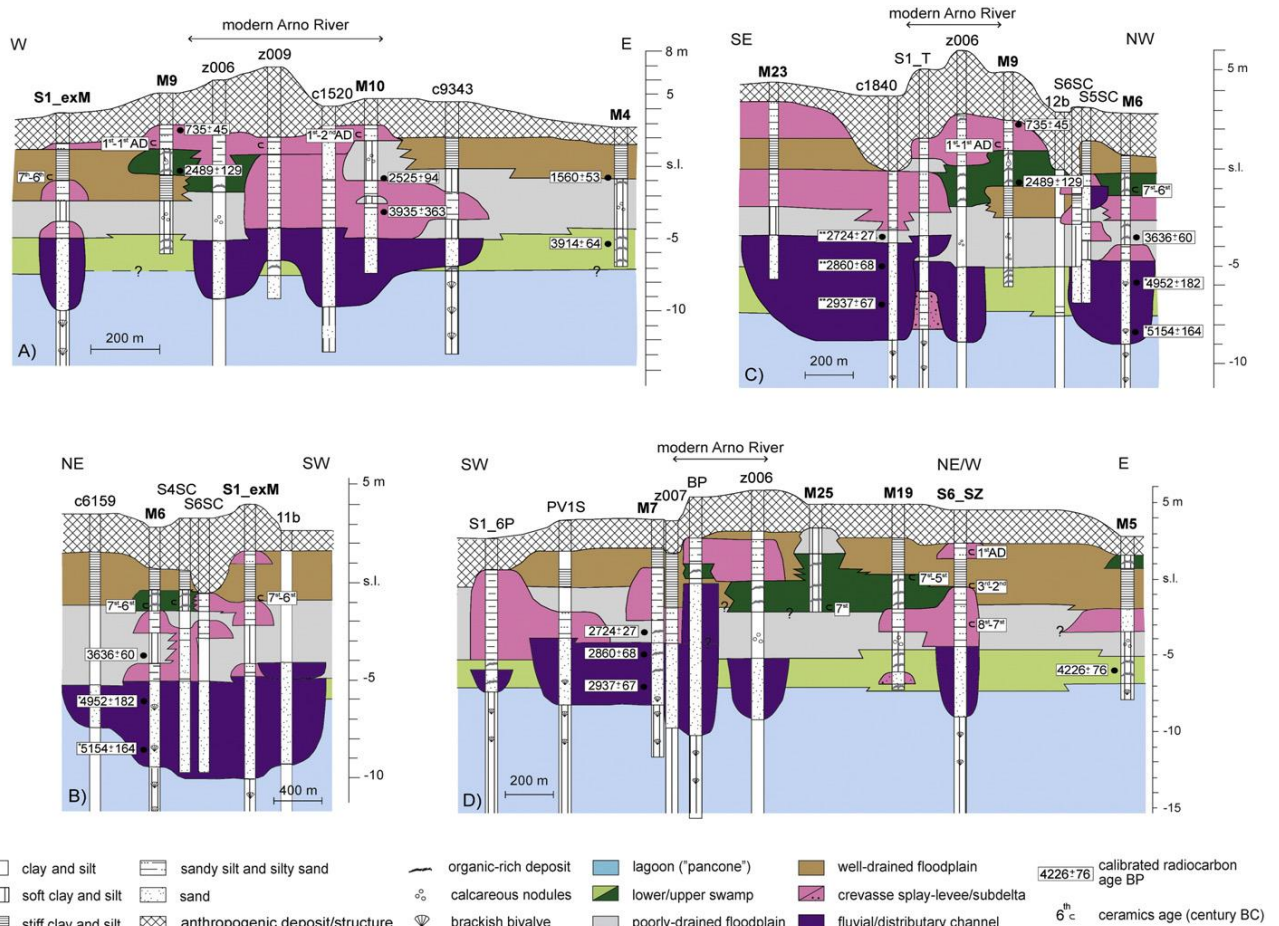


Fig. 3. Representative cross-sections depicting the mid-late Holocene lithofacies distribution and stratigraphic architecture of the deltaic-alluvial prograding wedge buried beneath the study area (section traces reported in Fig. 2). Reference MAPPA cores are in bold. Radiocarbon data are reported as calibrated yr BP (see Table 3), while the archeological data from A morose et al. (2013a) are reported in century BC/AD. Ages from reworked *Cardium* shells (asterisks) refer to lagoon environments pre-dating channel activity. Double asterisks indicate radiocarbon ages projected from core M7 (see Fig. 1 for location).



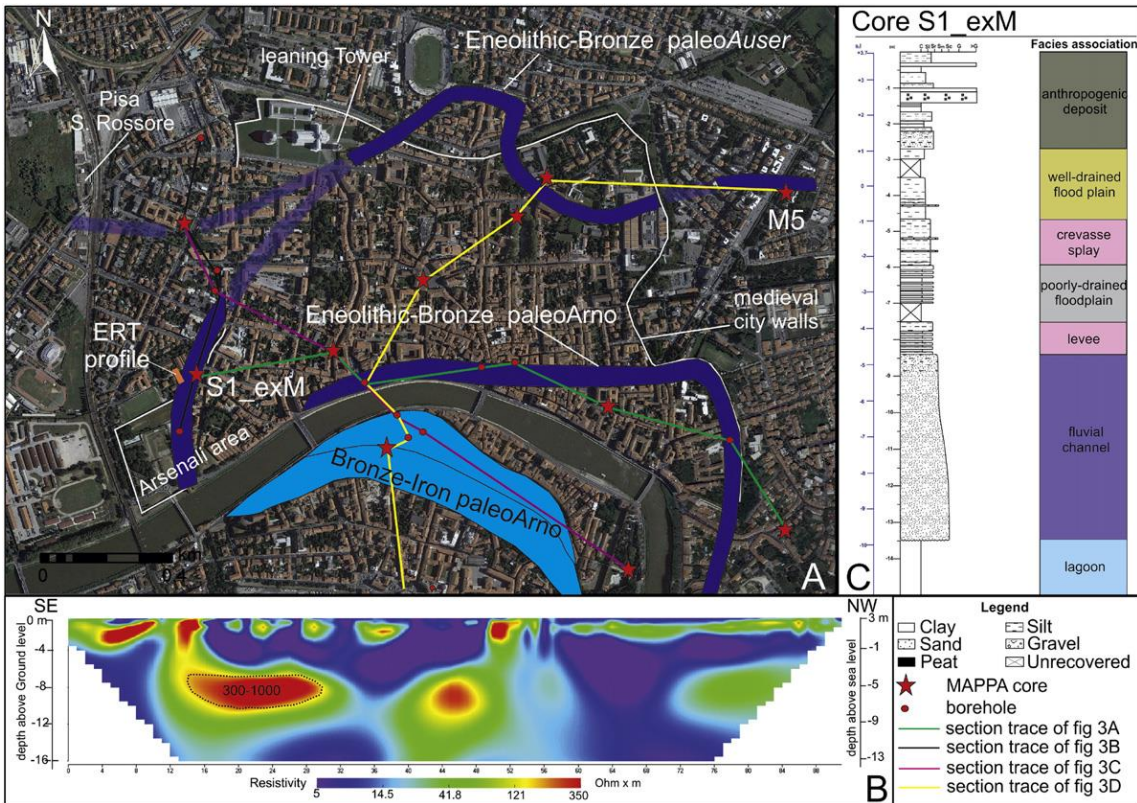


Fig. 4. A) Paleodrainage evolution of the Pisa Plain in proto-historic times (see Fig. 3A–D), reconstructed on the basis of integrated stratigraphic-remote sensing analyses. B) ERT profile and C) Core S1\_exM stratigraphy are also shown.

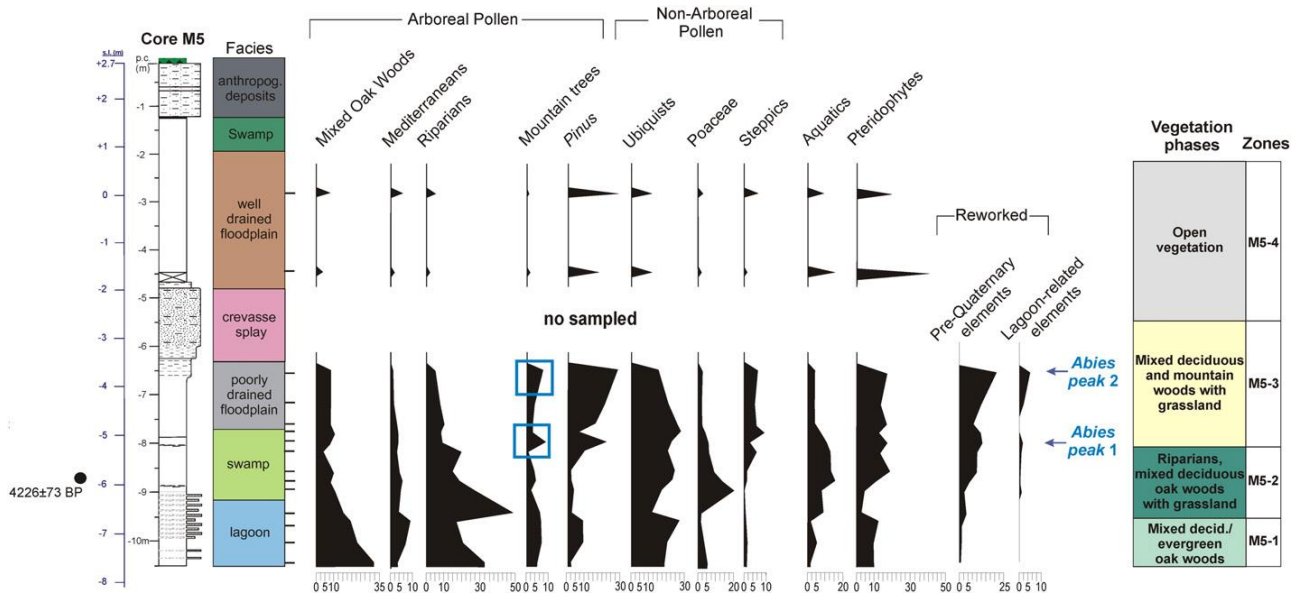


Fig. 5. Mid-late Holocene pollen record of core M5 (see Figs. 1 and 2 for location), with indication of the main vegetation phases/pollen zone (see Section 5 for more detailed information). The sandy interval (crevasse splay) is not sampled. Pollen taxa are grouped following Amorosi et al. (2009). Pollen concentration, AP/NAP ratio, pre-Quaternary and marine-related palynomorph percentages are also reported. Within zone M5-3, the *Abies* peaks 1 and 2 discussed in text are highlighted. Radiocarbon ages are reported as cal yr BP (see Table 3). For the lithological key of core M5 see Fig. 4. Lithofacies interpretation of core M5 is from Amorosi et al. (2013a); see Table 2 for more detailed facies information.

**Table 1**

Archeological chronology for the Pisa Plain (slight modified from <http://www.mappaproject.arch.unipi.it>).

Age	Chronology	Time range (yr BC/AD)	Time range (cal yr BP)
Prehistoric	Neolithic	(5500–3300 BC)	ca. (7500–5300)
Proto-historic	Eneolithic	(3300–1900 BC)	ca. (5300–3800)
	Bronze age	(1900–901 BC)	ca. (3800–2850)
Historical	Iron age	(900–721 BC)	ca. (2850–2700)
	Early Etruscan period	(720–481 BC)	ca. (2700–2400)
	Late Etruscan period	(480–90 BC)	ca. (2400–2000)
	Early Roman period	(89 BC–192 AD)	ca. (2000–1750)
	Late Roman period	(193–600 AD)	ca. (1750–1350)
	Early middle ages	(601–1000 AD)	ca. (1350–950)
	Late middle ages	(1001–1491 AD)	ca. (950–450)
	Modern age	(1492–1814 A)	ca. (450–150)
	Contemporary age	(1815 AD–present)	ca. (150–present)

**Table 2**

Diagnostic sedimentological and paleontological features and interpretation of the main lithofacies associations from the mid-late Holocene subsurface succession of the Pisa Plain depicted in Fig. 3 (from Amorosi et al., 2013a).

Lithofacies	Sedimentological features	Micropaleontological content	Palynological content
Fluvial/distributary channel	Gray to yellow-brown, fine- to coarse-grained sand bodies with erosional lower boundary and distinctive fining-upward trend	Barren or poorly-preserved marine, brackish foraminifers and ostracods	No sampled
Crevasse splay, levee and subdelta	Silty sand and fine sand with characteristic coarsening-upward trend (crevasse splay and subdelta) or rhythmical sand-silt alternation (levee). Scattered plant remains, wood and small-sized, unidentifiable mollusc fragments are present, along with rare calcareous nodules and yellow-brown mottles	Barren or poorly-preserved marine, brackish foraminifers and ostracods	No sampled
Well-drained floodplain	Dry, stiff, light brown silty clay with low organic-matter content and evidence of subaerial exposure, including indurated horizons, calcareous nodules and yellow-brown mottles, due to iron and manganese oxides	Barren	Dark-brown to brown reworked phytoclasts and heterogeneous continental palynomorphs with many reworked specimens
Poorly-drained floodplain	Monotonous succession of light gray, soft clay and silty clay, with scarce organic matter and isolated, large (up to 3 cm) calcareous nodules. Sharp-based cm- to dm-thick sand and silt layers occur. Scattered plant remains were encountered along with few, thin-shelled mollusc fragments	Barren or few valves of <i>P. albicans</i> or <i>C. torosa</i> , the latter within organic-rich layers	Rounded, dark brown to black phytoclasts, homogeneous in size with AOM, the latter sporadically abundant within organic-rich layers. Many reworked specimens derived from either ancient sediments or adjacent lands
Lower/upper swamp	Dark soft clay and silty clay, with local presence of cm- to dm-thick sand layers. Wood fragments and peat layers are very abundant. Scattered fragments and shells of freshwater gastropods are also recorded	Scarce oligotypic ostracod fauna mainly composed of <i>Pseudocardona albicans</i> and accompanied by rare <i>Candona neglecta</i> and <i>Ilyocypris</i> species	Abundant, light orange to brown/black phytoclasts (majority > 100 µm), AOM abundant
Lagoon ("pancone")	Monotonous succession of soft blue-gray clay and silty clay with abundant shells of <i>Cerastoderma glaucum</i> . Cm-thick fine sand intercalations. Wood and plant fragments scattered	Moderately to highly marine-influenced brackish water meiofauna, dominated by <i>Ammonia tepida</i> and <i>A. parkinsoniana</i> and <i>Cypridets torosa</i>	Orange-brown phytoclasts (<500 µm) and AOM – amorphous organic matter sporadically present, along with marine-related as dinocysts, foraminiferal linings and scolecodonts

**Table 3**

Radiocarbon chronology. List of the radiocarbon dates obtained from different core samples and discussed in this paper. Calibration has been performed using intcal09.14c (Reimer et al., 2009). Local reservoir correction  $\Delta R$  ( $35 \pm 42$ ) was applied to shell samples (*Cerastoderma glaucum* valves).

Code sample	Conventional age ( $^{14}\text{C}$ yr BP)	Calibrated age ( $^{14}\text{C}$ yr BP $\pm 2\sigma$ )	Material
M9_5.35	2456 $\pm$ 41	2360–2618	Wood fragment
M9_2.75	827 $\pm$ 23	690–780	Wood fragment
M10_7.85	3613 $\pm$ 137	3572–4298	Organic clay
M10_5.30	2465 $\pm$ 27	2525 $\pm$ 94	Wood fragment
M4_8.15	3610 $\pm$ 24	3850–3978	Wood fragment
M4_3.80	1642 $\pm$ 26	1507–1613	Soil
M6_10.75	4915 $\pm$ 35	4990–5318	Mollusc shells
M6_8.70	4708 $\pm$ 47	4770–5133	Mollusc shells
M6_6.04	3395 $\pm$ 25	3576–3696	Organic clay
M7_11.40	2843 $\pm$ 23	2870–3005	Wood fragment
M7_8.77	2773 $\pm$ 23	2792–2929	Wood fragment
M7_7.10	2559 $\pm$ 28	2697–2752	Wood fragment
M5_8.76	3842 $\pm$ 24	4153–4300	Organic clay
M3_5.75	3496 $\pm$ 27	3694–3840	Wood fragments

**Table 4**

Bronze–Iron age centennial flooding events in the Mediterranean regions based on  $^{14}\text{C}$ -dated Holocene fluvial deposits (modified after Benito et al., 2014).

Central Italy (this study)	Southern Italy (cal yr BP)	E-Iberian Peninsula (cal yr BP)	Southern France (cal yr BP)	Tunisia (cal yr BP)	Eastern Mediterranean (cal yr BP)
$\approx 3800$	4200–4100			4100–3700	4100–3700
	3450–3000				
$\approx 2900$ –2800			3000–2750	3300–3000	3400–3200
	2350–1850	2850–2700 2450–2150	2300–1750	2850–2350	